PERGAMON

Planetary and Space Science 49 (2001) 1437–1444

Planetary and Space Science

www.elsevier.com/locate/planspasci

Capability of solar electric propulsion for planetary missions

Giuseppe D. Racca *

Scientific Projects Department, ESA/ESTEC, Keplerlaan 1, 2200AG Noordwijk, Netherlands

Received 27 July 2000; accepted 27 September 2000

Abstract

Historically, deep space exploration was initiated by a series of flyby missions that were propulsively and energetically modest. The basic energy barrier given by the use of chemical propulsion system was not a limiting factor. Later on, the use of *gravity assists* has enabled missions with enlarged velocity increments. Unfortunately, multiple gravity assists have the drawback to narrow dramatically the launch windows. Moreover, the cruise phases are extremely long with obvious impacts on the operation costs. The most promising solution for the future deep space missions is found in the use of the electric propulsion (EP). Owing to its high specific impulse, the EP enables very high velocity increments, higher payload ratios and the use of smaller launchers. In addition it allows to have more flexible launch windows and ultimately reduces the cruise time.

Europe possesses a variety of EP systems. Two main parameters characterise the performance of these EP systems: the specific impulse and the specific power. The first parameter is a measure of the fuel consumption, while the second is the main design driver for the on board power system. The increase in specific impulse enables missions requiring a large ΔV. However, in practice the maximum ΔV is limited to some 10 km/s, while a typical EP-based mission to Mercury requires 16 km/s. Hence, trajectories combining both *low-trust* and *gravity-assist* techniques have been devised for the ESA's BepiColombo mission.

SMART-1 is a precursor mission to test these system and mission aspects.

1. Introduction

The planetary exploration performed by man-made probes began in 1959 with the Soviet Luna 1, 2 and 3 and the American Pioneer 4 to the Moon. The exploration of the inner solar system continued then in the 1960s and early 1970s with the US Mariner series to Venus, Mars and Mercury, the Soviet Zond to the Moon, the US Ranger, Lunar Orbiter, Surveyor and Apollo series to the Moon and Soviet Venera to Venus.

The outer planets' exploration started with the American Pioneer 10 in 1972 to Jupiter followed by Pioneer 11 in 1973. The probes Voyager 1 and 2 to Jupiter, Saturn, Uranus and Neptune were launched in 1977. The visits to the inner solar system planets continued with Viking in 1975 to land on Mars and in 1978 NASA launched Pioneer Venus orbiter and multiprobe. Missions targeting minor bodies were launched by US, ISEE-3 to comet Giacobini–Zinner in 1978 and by the Soviets in 1984 with Vega 1 and 2 to Halley's comet, also flybying Venus and ESA's Giotto and Japanese Sakigake and Suisei to Halley in 1985. Two Soviet Phobos to Mars were launched in 1988, Galileo was launched in 1989 to Jupiter via Gaspra and Ida asteroids, Magellan to Venus in 1989, the Japanese Hiten to the Moon in 1990 and ESA/NASA Ulysses, launched in 1990, flew by Jupiter before heading into a polar orbit around the sun.

The last decade started with the loss on Mars Observer, launched in 1992, however Clementine managed to orbit the Moon in 1994. In 1996, American NEAR was launched towards the Mathylda and Eros asteroids and Mars Global Surveyor and Pathfinder were launched towards Mars. In the same year the Russian Mars 96 failed at launch. The NASA/ESA mission to Saturn and satellite Titan Cassini–Huygens was launched in 1997. The US Lunar Prospector orbited the Moon in 1998 and in the same year Deep Space 1 was launched targeting an asteroid and a comet. The Japanese Nozomi was also sent to Mars in 1998, but the arrival is now scheduled by 2003. Two missions failed, in 1998 and 1999, Mars Climate Orbiter and Mars Polar Lander, which was also carrying the Deep Space 2 penetrators, before the successful launch in 1999 of the US Stardust comet coma sample return mission.

To date, except Pluto–Charon, all the planets and a number of the main solar system bodies have been visited. It can

* Tel.: +31-71-565-4618; fax: +31-71-565-5770.
E-mail address: gracca@estec.esa.nl (G.D. Racca).

0032-0633/01/$ - see front matter
PII: S0032-0633(01)00084-8

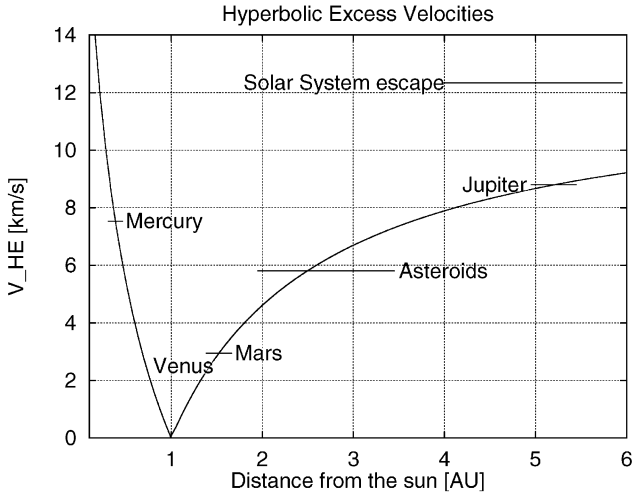

Fig. 1. Hyperbolic excess velocity plot versus the helispheric distance in AU. The planet positions is shown as a horizontal bar covering the range of distances from the sun assumed by the planet in its orbit. The vertical position of the line shows the average required V_{HE}. The line labelled *Solar System escape* is positioned at $V_{HE} = 12.34\ km^{-1}$ and signifies the required hyperbolic excess velocity to escape the gravitational attraction of the sun and reach the interstellar space.

be concluded that the solar system exploration is well underway. However, there are intrinsic limitations to this type of wandering among the planets. With the exception of Deep Space 1, all the above missions have been accomplished by means of conventional chemical propulsion means which have hard limitations. This problem is analysed in more detail in the next section.

2. The energy problem

2.1. Minimum energy trajectory

In order to illustrate the problem of how much energy is required to reach points in the Solar System from the Earth, it is useful to consider the hyperbolic excess velocity V_{HE} required by a spacecraft to reach a planet's orbit with semimajor axis a_p. This is the velocity required in addition to the Earth's heliospheric velocity $V_\oplus = 29.79$ km/s

$$V_{HE} = V_\oplus \left| \sqrt{\frac{2a_p}{a_\oplus + a_p}} - 1 \right|, \tag{1}$$

where $a_\oplus = 1$ astronomical unit (AU) is the mean radius of the Earth's orbit. Eq. (1) is plotted as a function of a_p in Fig. 1. The V_{HE} value in Fig. 1 gives an indication of the difficulty to reach the various planets. For example, it can be seen that the easiest to reach is Venus, while Mercury is roughly as difficult as Jupiter. Approaching the sun is in turn more difficult than escaping the Solar System.

The mission requirements in terms of ΔV are usually specified to the launcher in terms of the parameter C_3, which is twice the vis-viva energy per unit mass of the spacecraft. C_3 is the square of the hyperbolic excess speed of the Earth escape trajectory, i.e. $C_3 = V_{HE}^2$. Alternatively to the direct injection, the travel to the planet positions can be performed by the spacecraft own engines starting from an Earth parking orbit, of perigee radius ρ_o. The selection of the perigee as a departing point is made to take advantage of the higher velocity at that point, however, in principle the departing hyperbola need not to start from a parking orbit perigee. The radius of the Earth's outer sphere of influence is $\rho = 2.66 \times 10^6$ km. In order to provide the spacecraft with a certain V_{HE} at the limit of the Earth's sphere of influence, a δV has to be provided by an on-board engine, as per Eq. (2)

$$\delta V = \sqrt{V_{HE}^2 + 2\mu_\oplus \left(\frac{1}{\rho_o} - \frac{1}{\rho} \right)} - V_p, \tag{2}$$

where V_p is the velocity of the spacecraft at perigee and $\mu_\oplus$ is equal to the product of the universal gravitational constant G and the Earth mass and is equal to $3.986 \times 10^5\ km^3/s^2$. Eq. (2) gives the velocity impulse that will bring the spacecraft to the planet orbit by means of a Hohmann transfer manoeuvre. This can also be considered for all practical purposes [1] as the minimum required velocity impulse.

If we consider a circular parking orbit with an altitude of 185 km, we obtain the values of the second column of Table 1. Once the spacecraft has reached the desired planet's orbit and has entered its sphere of influence, it will possess a hyperbolic excess velocity expressed by Eq. (1) by replacing $V_\oplus$ with the planet's heliospheric velocity. This excess velocity will have to be cancelled by another velocity impulse given by the on-board engine. In order to inject the spacecraft into an orbit around the planet, the δV at the planet can also be expressed by the same Eq. (2), by replacing the relevant gravitational parameter and orbit radii of the Earth with those of the planet. If we consider to orbit the planet circularly at an altitude equal to 10% of the planet's radius, we obtain the δV values of the third column of Table 1.

The total mission velocity increment is hence given by the sum of the two columns, as shown in the fourth column. By examining the values displayed, one realises that they are indeed quite large for all mission cases. Except Mars and Venus and the Solar System escape, all missions require more than 10 km/s which is provided by the on-board engine. The velocity increment can be easily translated into a propellant mass ratio R needed to impart that ΔV to a certain total spacecraft mass m, once it is known the specific impulse I_{sp} of the engine is used to produce the impulse. The following rocket equation can be written, where g is the

[1] The classical Hohmann transfer gives the minimum total δV only for critical ratios of final to initial orbit radii lower than 11.93876. For greater ratios, other manoeuvres like bi-elliptical transfers, require less ΔV, but employ a considerably longer transfer time.

Table 1
Comparison of energy requirements for different planetary missions[a]

Planet	ΔV_e (km/s)	ΔV_p (km/s)	$\Delta V_e + \Delta V_p$ (km/s)	Useful mass ratio (%) for different I_{sp}[s]		
				300	1500	3000
Mercury	5.56	7.56	13.12	1.16	41.00	64.03
Venus	3.51	3.26	6.77	10.02	63.12	79.45
Mars	3.62	2.08	5.7	14.42	67.88	82.39
Jupiter	6.31	16.98	23.29	0.04	20.54	45.32
Saturn	7.29	10.36	17.65	0.25	30.14	54.90
Uranus	7.98	6.51	14.49	0.73	37.35	61.12
Neptune	8.25	6.90	15.15	0.58	35.72	59.76
Pluto	8.36	5.68	14.04	0.85	38.51	62.06
Sun 3R	19.44		19.44	0.14	26.68	51.66
Escape	8.75		8.75	5.11	55.18	74.28

[a]ΔV_e is the impulse to be given at the Earth circular orbit of 185 km, ΔV_p is the impulse to be given at the planet to insert the spacecraft into a circular orbit of radius 1.1 times the planet radius. The "Sun 3R" stands for a solar orbit at 3 solar radii altitude. For comparison the ΔV required to pass from a 185 km circular altitude to a Standard Geotransfer orbit (GTO) which is about 2.5 km/s. Therefore, if a spacecraft is parked in a GTO, the ΔV requirement has to be reduced of 2.5 km/s.

Earth's gravitational acceleration:

$$R = \frac{\Delta m}{m} = 1 - e^{-\Delta V/I_{sp}g}. \quad (3)$$

It follows naturally that the value $1 - R$ is the dry mass ratio, i.e. all that is in the spacecraft need not be propellant, sometimes called also as *useful mass ratio*. The specific impulse is the amount of impulse that can be given by a certain engine with a unit mass of propellant. This is a characteristic of the type of engine and propellant used. Its numerical value is usually expressed in seconds, in engineering unit. For spacecraft main chemical propulsion the specific impulse takes values around 300 s. Electric propulsion, as we shall see later, can produce specific impulses in the range 1500–3000 s or higher, depending on the technology.

The last three columns of Table 1 show the useful mass ratios in percentage for different specific impulses and for the mission cases. The fifth column clearly shows that no missions of this type can be accomplished by using chemical propulsion. The easiest mission is to orbit Mars, but even in this case almost 85% of the spacecraft mass has to be fuel. This seems to be quite in contradiction with the simple evidence of the many Mars missions flown so far. Indeed, apart from the different launch strategies (direct injections by a launch vehicle, as in the case for the Mars missions) many of the orbiting planetary missions make use of a powerful technique: the *gravity assist* or *planet swing-by*. The spacecrafts which intentionally first used this technique were Mariner 10 to Venus and Mercury and Pioneer 11 to Jupiter and Saturn.

2.2. Gravity-assist techniques

It is not the scope of this paper to describe the principle and techniques of the gravity assist manoeuvres, Broucke (1988) and Cornelisse et al. (1979) which provide a good background. The basic principles of the gravity-assist concept have been well known to astronomers for many years in relation to the capture and escape of comets due to Jupiter's action.

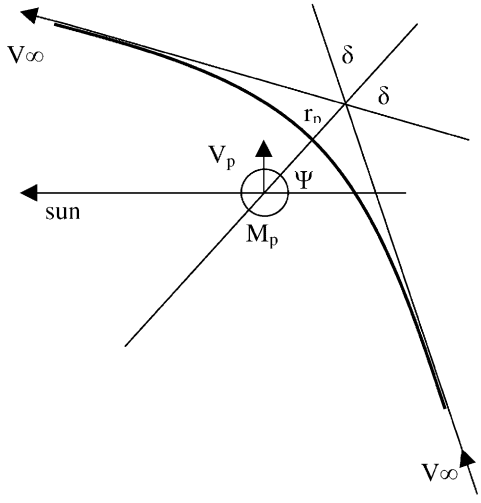

Fig. 2. Gravity-assist geometry.

To a very good approximation a spacecraft moves in a Keplerian orbit around the Sun. This orbit is likely to be elliptical, but it could also by a hyperbolic trajectory. With respect to Fig. 2, the gravity assist is the modification or perturbation of this Keplerian orbit when the spacecraft has a close approach to the planet of mass M_p. The change in the energy of the spacecraft orbit caused by the planet is given by Eq. (4).

$$\Delta E = -2V_P V_\infty \sin\Psi \sin\delta. \quad (4)$$

When the flyby is in front of the planet, there is a loss of energy, while when the flyby is behind the planet there is an increase of energy. In both cases the orbit is perturbed in a significant way, depending on the parameters of Eq. (4). The spacecraft enters into the planet sphere of influence with

a hyperbolic excess velocity V_∞ and exits it with the same velocity but deflected in an angle δ. It can be demonstrated that an optimum value exists for V_∞ and δ such that the gain in energy, or ΔV, is maximum. In this case, the ΔV provided by the gravity assist is given by Eq. (5)

$$\Delta V = \sqrt{\frac{\mu_p}{r_p}}. \tag{5}$$

Thus, the ΔV gained is equal to the circular velocity at the planet periapsis. The drawback of the gravity-assist techniques, especially in the case of multiple swing-bys, is the required long cruise time. As an example, Hechler (1996) computed Mercury orbiter missions of launch dated for July 2004 multiple VV–MM-GA (Venus–Venus–Mercury–Mercury gravity assist) trajectory which could save about 5.2 km/s, at the expense of a time of flight of 3.78 yr, compared with mere 0.29 yr required by a Hohmann transfer. Even more can be saved, but again at the expense of additional cruise time.

Further techniques exist which improve even further the gravity-assist manoeuvres. The first technique, called *powered flyby* and sometimes identified as ΔV GA, consists in enhancing the swing-by by applying an additional ΔV by means of an engine burn in the vicinity of the planet.

Another method, dubbed V_∞ *leveraging*, is a technique to increase the V_∞ by performing a small manoeuvre at apoapsis which gives a great payback at the following planet flyby. The third method consists of further enhancement of the gravitational effect by introducing *aerobraking*, e.g. flying through the upper atmosphere of a planet, like the Earth, Mars or Venus. The manoeuvre results in increasing the deflection angle δ by obtaining a lift force in the atmosphere to balance the centrifugal force and hence fly at a constant altitude. A disadvantage is that the co-existing drag forces reduce the speed V_∞. Hence, there is a need to minimise the drag losses $\delta V_\infty / V_\infty$. Moreover, the technological problems of hyperbolic flight, with speed of more than 25 km/s, pose serious constraints. This technique was first used by the Magellan spacecraft in 1993 to change its orbit around Venus.

The conclusion of this section is that despite enhancing techniques like gravity and aero assists, conventional propulsion shows limitations for planetary exploration both in terms of energy and time of flight. Indeed this limitation was recognised already in the 1960s and 1970s, studies on alternatives were carried out.

Electric propulsion and *solar sail* seemed to be the most promising techniques for flying fast and efficiently in space. Solar sail techniques have been investigated and partially tested also in space, but presently are not yet considered a mature candidate. As a matter of fact solar and nuclear electric propulsion has been considered to be the near term candidates. Nuclear electric propulsion has been extensively studied in the US and in Europe (Loeb and Popov 1995), but due to its political and social difficulties it is presently not considered a near term concrete alternative. Therefore, the solar electric propulsion is the key technology considered in this paper.

3. Solar electric propulsion

Solar electric propulsion is a system which uses the electrical energy, produced by the photovoltaic cells array, to accelerate to a great speed the atoms of a gas used as propellant. Saccoccia and Gonzalez (1994) report a comparative analysis of the applicability of different types of low-power electric propulsion technologies to current and future space missions. Schematically, the electric propulsion engines can be subdivided into three categories:

- *Electrostatic thrusters*: where the propellant once ionised is accelerated by an electrostatic field generated with various techniques. Examples of these thrusters are the *Ion engines*, the stationary plasma thrusters (SPT) and the field emission electric propulsion (FEEP) thrusters.
- *Electrothermal thrusters*: where the gas is heated by electrical energy and accelerated by gasdynamic expansion in a nozzle. Examples of such thrusters are the *Arcjets* and *Resistojets*.
- *Electromagnetic thrusters*: where the electrical energy is used to create a neutral plasma, which is subsequently expelled at high velocity by the interaction of the discharge current with a magnetic field. An example of these thrusters is the *Pulsed* magneto-plasma dynamics (MPD) thruster.

The choice among the different propulsion concepts is driven by various mission requirements and constraints. In this paper, only the *electrostatic thrusters* are considered further, as they are more relevant to the planetary missions.

In an electrostatic thruster, the gas has to be electrically charged in order to be accelerated, hence it is first ionised, thus a plasma is created and maintained. The ions are accelerated by means of an electric field and finally the plasma is neutralised again by injection of electrons. According to the mechanism of plasma production, maintenance and acceleration, three types of electric propulsion engines can be identified.

3.1. Stationary plasma thruster

Stationary plasma thrusters form a family of electric propulsion engines belonging to the category of "Hall-effect Thrusters". The schematic of this type of thrusters is shown in Fig. 3. Electrons from an external cathode enter a ceramic discharge chamber, attracted by an anode piece. On their way to the anode, the electrons encounter a radial magnetic field created between inner and outer coils, causing cyclotron motion around the magnetic field lines. Collisions between drifting electrons and Xenon propellant create the

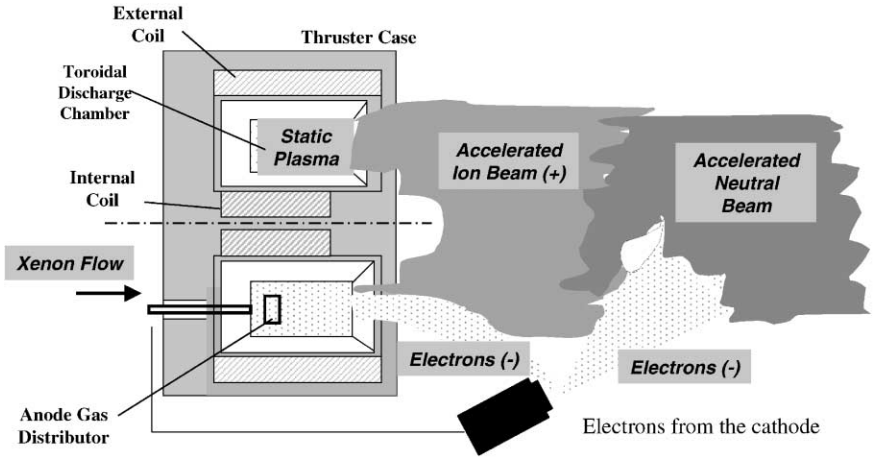

Fig. 3. Schematic of a stationary plasma thruster.

plasma. The ions created are accelerated by the negative potential existing in the area near the exit of the chamber due to the Hall-effect. The external cathode acts also as a neutraliser, injecting electrons into the beam, in order to maintain zero-charge equilibrium in the thrust beam and on the spacecraft. The PPS1350 has an exit diameter of 100 mm and provides a nominal thrust of 70 mN at 1640 s specific impulse (Isp) and with 1350 W of nominal input power. The thruster can also work at reduced power. This type of thruster has been already qualified for 7000 h of operations in cycles (corresponding to a total impulse of 2 MN s).

3.2. Radio-frequency ionisation thrusters

Radio-frequency ionisation thrusters belong to the category of ion engines. In these thrusters, see schematic in Fig. 4, the Xenon propellant flows inside a ceramic discharge chamber through the extraction anode, which also functions as a gas distributor. The discharge chamber is surrounded by an induction coil connected to an RF-generator. Free electrons within the Xenon gas collect energy from the RF-induced electric field and ionise the neutral propellant atoms by inelastic collisions. The discharge is ignited by the injection of electrons from the neutraliser. Thrust is generated by the acceleration of ions in the electrostatic field applied to an extraction system comprising the extraction anode and a 3-grid system. The negative potential of the grids accelerates the positive ions out of the static plasma. A neutraliser injects electrons into the beam, to maintain zero-charge equilibrium in the beam and on the spacecraft. The RIT-10 has an exit diameter of 100 mm and provides a maximum thrust of 23 mN at 3060 s Isp for an input power of 700 W. Thrust can be modulated. The thruster is being qualified for 15000 h of operations in cycles (corresponding to a total impulse of 1 MN s) at 15 mN level.

3.3. Electron bombardment ionisation thrusters

Electron bombardment ionisation thrusters belong to the category of ion engines. In these thrusters, see schematic in Fig. 5, the Xenon propellant flows inside a ceramic discharge chamber through a gas distributor. Free electrons produced by a cathode inside the chamber are attracted by an anode pole at the end of the chamber and flow along magnetic field lines created by a number of electromagnetic coils surrounding the chamber. Along this path, the electrons hit the propellant atoms and ionise them. Thrust is generated by the acceleration of the ions in the electrostatic field applied to an extraction system comprising the extraction anode and a 3-grid system. The negative potential of the grids accelerates the positive ions out of the static plasma. A neutraliser injects electrons into the beam, to maintain zero-charge equilibrium in the beam and on the spacecraft. The UK-10 has an exit diameter of 100 mm and the current version of the thruster provides a maximum thrust of 23 mN at 3400 s of Isp for an input power of 700 W. Thrust can be modulated.

From the above sections, one sees that the basic characteristic of the *gridded* engines (i.e. electron bombardment ionisation and radio-frequency ionisation thrusters) is to have a very large specific impulse, in the order of 3000 s or more and a relatively high power consumption per unit thrust, in the order of 30 W/mN. The *plasma* engines (i.e. stationary plasma thruster) instead exhibit a specific impulse in the order of 1600 s and a relatively modest power consumption, in the order of 20 W/mN. The question of what engine is best suited for a particular application is not trivial. Indeed many parameters have to be considered, including also the cost. Before passing to more detailed considerations on the advantages of high specific impulse versus high thrust, it is necessary to understand the types of trajectories that can be flown by means of an electric propulsion engine.

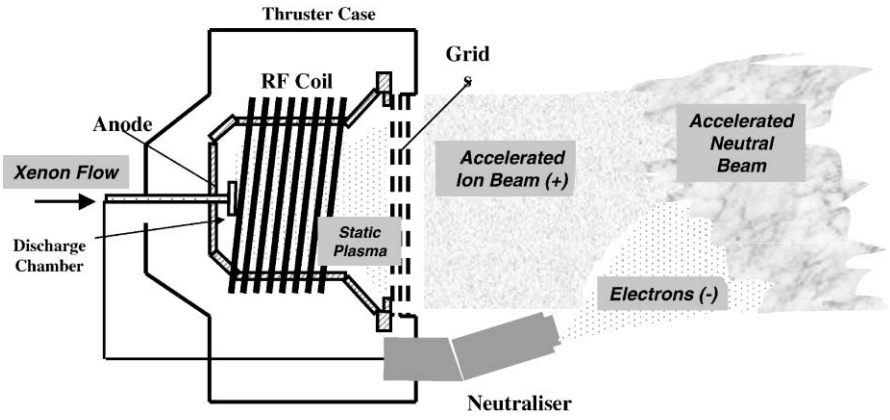

Fig. 4. Schematic radio-frequency ionisation thruster.

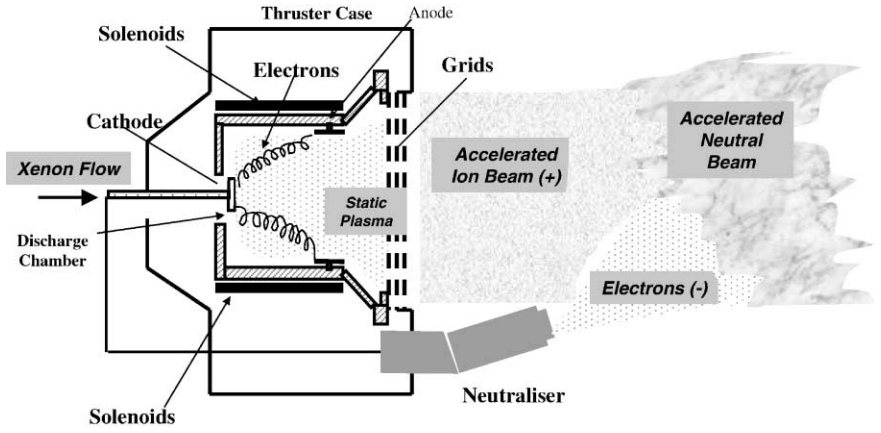

Fig. 5. Schematic of an electron bombardment thruster.

4. Low-thrust trajectories

The thrust provided by an electric propulsion engine is, in general, very low. Thus, the acceleration imparted to the spacecraft is low and it is necessary to thrust for a long time in order to obtain a given ΔV. In Section 2 only Hohmann transfers, minimum energy manoeuvres have been considered. In these manoeuvres, the various ΔV's are assumed to be given by the engine burn in a timeless instant, so that during the time of the burn the orbital parameters do not vary considerably. If this approximation is acceptable for spacecraft mass-to-thrust ratio of about 1 kg/N, it is definitely not valid when the mass-to-thrust ratio increases by 3 or 4 orders of magnitude. As a consequence the trajectory flown will not be a "minimum energy" one. Indeed a *low-thrust trajectory* will be flown, where the thrust is given for long arcs of the orbits.

The optimisation of low-thrust trajectories has been studied by ESA extensively in the early 1980s. More recently, with the advent of real missions based on electric propulsion, the problem has been tackled again in a more operational fashion. Jehn et al. (2000) describe the optimisation methods currently used by ESA/ESOC. Many techniques are based on the Pontryagin maximum principle (Jehn and Cano, 1999). The methods used by ESOC for the calculation of the SMART-1 trajectory (Racca et al., 2001) rely on a technique by Geffroy (1997) to solve the associated boundary value problem and on other approximate methods (Pulido Cobo and Schoenmaekers, 2000). The solution to the problem is a trajectory which combines coast and thrust arcs. During the thrust arcs, the engine is fired in a direction which has a out-of-plane and in-plane component with respect to the velocity vector.

In general, the optimised trajectory obtained will be different according to the type of engine (its specific impulse and thrust) and will require more or less ΔV to be provided by the electric propulsion system. Therefore, although it is clear that a higher specific impulse provides a lower propellant consumption, it is not always obvious how much this advantage is offset by the increase of ΔV that a lower thrust implies.

In order to illustrate this important fact a simple example is made. If the purpose of a manoeuvre is to increase the semimajor axis of an initial elliptical orbit, we can use

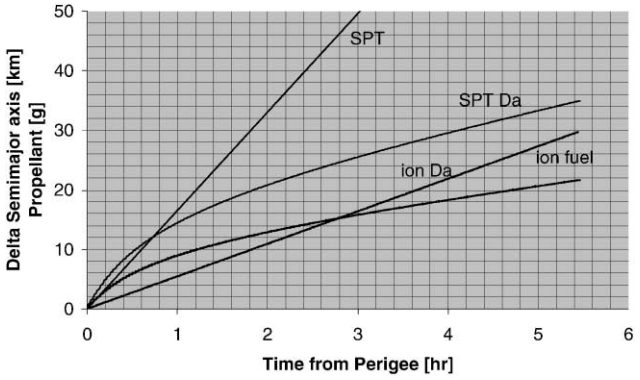

Fig. 6. Plot of the Δa obtained with the two types of electric propulsion engines: SPT and ion (or gridded). On the same scale the amount of fuel in grams is also plotted. The burn starts at perigee and continues up to apogee.

the time derivatives of semimajor axis a from Lagrange's planetary equation

$$\frac{\mathrm{d}a}{\mathrm{d}t} = \frac{2a^2}{\sqrt{\mu a(1-e^2)}}\left[Se\sin\theta + C\frac{a(1-e^2)}{r}\right], \qquad (6)$$

where θ is the true anomaly, r is the local radius, $S=(F/M)\sin\delta$ is the electric propulsion acceleration along the radius and $C=(F/M)\cos\delta$ is the acceleration perpendicular to the radius, positive in the sense of motion. Let us suppose that the thrust is oriented perpendicularly to the radius, so that $S=0$ and $C=(F/M)=\dot{m}I_{\mathrm{sp}}g/M$. The mass flow rate $\dot{m}$ is kept constant during the flight and depends on the type of engine and power available. By integrating the Eq. (6), we obtain an expression for the change of semimajor axis during a continuous burn of time T

$$\Delta a = \frac{2a^2}{\sqrt{\mu a(1-e^2)}}\frac{F}{M}\int_0^T (1+e\cos\theta(t))\,\mathrm{d}t, \qquad (7)$$

where the true anomaly θ is related to the time from perigee through the eccentricity anomaly. If we insert the orbital elements of a geostationary transfer orbit and the SMART-1 spacecraft mass $M=350$ kg and 1400 W power to the electric propulsion, we can integrate Eq. (7) and plot the results in Fig. 6 for a plasma engine and a gridded engine.

Let us suppose that the intention was to increase 22 km, the semimajor axis by this thrust strategy. We see that this would be obtained either with a plasma thruster in 2.2 h and with a Xe propellant consumption of 35 g, or with a gridded ion engine in 5.5 h of thrust and with a Xe propellant consumption of 30 g. This proves, what is stated above, that the high specific impulse is not the only parameter to be looked at in evaluating the most suitable thruster for a given mission. The plasma thuster offers in this case much more time for other non-propulsive activities, for a modestly higher propellant use.

However, when the total mission ΔV demand becomes above a certain value (typically 10 km/s) the employment of plasma thruster becomes rather difficult, as the relatively low specific impulse, leaves only less than 50% of the useful mass ratio (see Table 1).

Moreover, if the ΔV is very large ($\gg 15$ km/s), today's gridded engines become inadequate.

The BepiColombo interplanetary trajectory design, described in ESA-SCI (2000), started from the consideration, derived from previous studies, that direct low thrust transfer to Mercury typically require a ΔV of about 16 km/s for an optimum launch escape velocity of 2 km/s. Such large values rule out completely the use of SPT engines and even with ion engine the dry mass of the spacecraft would be only 55% of the total mass. In addition the thrusters would have to operate continuously for about 17,000 h, which would also make the employment of existing grid technology rather doubtful. As a consequence, the direct mission option was ruled out. A similar path was then followed as for the chemical propulsion missions: gravity assist combined with electric propulsion. This missions devised by Langevin (1999) proved to be the winning strategy for the BepiColombo mission. This strategy provides the best compromise between the mass budget and the cruise time. Indeed by means of a multiple Venus gravity assist the ΔV requirement reduced to about 7 km/s for a total cruise time of 2.6 yr.

5. Conclusions

The planetary exploration has started with missions requiring modest energy, essentially based on chemical propulsion. Subsequently, techniques like gravity assist has allowed many missions to be performed. However, a hard limitation is currently hit for the most demanding missions, like Mercury orbiting or landing missions or solar probes and close solar orbiters. Alternative means have been studied and the currently most advanced and promising one is the solar electric proplusion. For moderate ΔV (3–8 km/s) both plasma thruster and gridded ion engines can be used, while for more energetic missions, gridded ion engines are the obvious choice. Electric propulsion alone, however, does not solve all problems, but its combination with gravity assists has proved to be a viable solution.

The SMART-1 mission (Racca et al., 2001) is specifically designed to test all these techniques to be later applied on BepiColombo and other solar system missions.

Acknowledgement

The author wishes to acknowledge the contribution to this paper by the experts of the Electric Propulsion Section of ESTEC, headed by G. Saccoccia, for providing data on the electric propulsion technologies.

References

Broucke, R.A., 1988. The celestial mechanics of the gravity assist, AIAA paper 88-4220-CP.

Cornelisse, J.W., Schöyer, Wakker, K.F., 1979. Rocket Propulsion and Spacecraft Dynamics. Pitman Publishing Limited, London.

ESA-SCI, 2000. BepiColombo, System and Technology Study Report. ESA- SCI(2000)1, Noordwijk, The Netherlands, April.

Geffroy, S., 1997. Généralisation des techniques de Moyennation en Contrôle Optimal—Application aux problème de Transfert et Rendez-Vous Orbitaux à Pousée Faible, Doctoral Thesis at CNES, Toulouse, France.

Hechler, M., 1996. Mercury orbiter mission analysis: on mission opportunities with chemical and solar electric propulsion. ESOC MAS Working Paper No. 389, Darmstadt, Germany.

Jehn, R., Cano, J.L., 1999. Optimum low thrust transfer between two orbits. MAS-WP No. 414, ESOC, Darmstadt, Germany, March.

Jehn, R., Hechler, M., Rodriguez-Canabal, J., Schoenmaekers, J., Cano, J.L., 2000. Trajectory optimisation for ESA low-thrust interplanetary and lunar missions. CNES Workshop on Low-Thrust Trajectory Optimisation, Toulouse, France, 7–8 March.

Langevin, Y., 1999. Chemical and solar electric propulsion options for a Cornerstone mission to Mercury. 50th IAF Congress, Paper IAF-99-A.2.04. Amsterdam, The Netherlands, 4–8 October.

Loeb, H.W., Popov, G.A. (Eds.), 1995. Advanced interplanetary missions using nuclear-electric propulsion. Joint Study Group Report. Giessen, Germany.

Pulido Cobo, J., Schoenmaekers, J., 2000. The gradient method adapted for SMART-1 trajectory optimisation. S1-ESC-RP-5502, ESOC, Darmstadt, Germany, April.

Racca, G.D., Foing, B.H, Coradini, M., 2001. SMART-1: the first time of Europe to the Moon. Earth, Moon and Planets 85, 379–390.

Saccoccia, G., Gonzalez, J., 1994. Electric propulsion technologies comparative analysis: application to current and future space missions. AIAA Paper 94-2860, 30th AIAA/ASME/SAE/ASEE Joint Propulsion Conference, Indianapolis, IN, June.